PHYSICAL REVIEW B **88**, 180101(R) (2013)

Origins of large enhancement in electromechanical coupling for nonpolar directions in ferroelectric $BaTiO_3$

A. Pramanick,[1,*] S. O. Diallo,[2] O. Delaire,[3] S. Calder,[2] A. D. Christianson,[2] X.-L. Wang,[4] and J. A. Fernandez-Baca[2]

[1]*Chemical and Engineering Materials Science Division, Oak Ridge National Laboratory, Oak Ridge, Tennessee 37831, USA*

[2]*Quantum Condensed Matter Division, Oak Ridge National Laboratory, Oak Ridge, Tennessee 37831, USA*

[3]*Materials Science and Technology Division, Oak Ridge National Laboratory, Oak Ridge, Tennessee 37831, USA*

[4]*Department of Physics and Materials Science, City University of Hong Kong, Tat Chee Avenue, Kowloon, Hong Kong SAR*

(Received 15 April 2013; revised manuscript received 13 September 2013; published 15 November 2013)

The origins of enhanced piezoelectric coupling along nonpolar crystallographic directions in ferroelectric $BaTiO_3$ are investigated using *in situ* neutron spectroscopy. It is observed that an electric field applied away from the equilibrium polarization direction causes a stiffening of the transverse acoustic (TA) phonon branch and consequently increases interaction between the TA and the transverse optic soft mode for a range of wave vectors extending from the Brillouin zone center. This provides a direct lattice dynamics mechanism for enhanced electromechanical coupling, and could act as a guide for designing improved piezoelectric materials.

DOI: 10.1103/PhysRevB.88.180101 PACS number(s): 77.80.−e, 78.70.Nx

Piezoelectric materials are attractive for their electromechanical coupling properties and are widely used in applications ranging from diagnostic medical imaging, to sonar, precision actuators, telecommunications, and energy harvesting.[1] The electromechanical properties of a material are often characterized by the piezoelectric coefficient d, which is the ratio between the resulting mechanical strain and the applied electric field which causes it. In certain ferroelectric single crystals and grain-oriented ceramics, d is dramatically enhanced for specific applied electric field directions that are different from the spontaneous polarization vector of the crystal lattice.[2–4] A detailed understanding of the origins for such enhancement has remained elusive. For example, in relaxor ferroelectric crystals $Pb(Zn_{1/3}Nb_{2/3})O_3$-$PbTiO_3$ with compositions close to the morphotropic phase boundary (MPB), a maximum $d_{33} \sim 2500$ pm/V is observed for applied electric fields along $\langle 001 \rangle$, while $d_{33} \sim 100$ pm/V when the electric field is applied parallel to the polar $\langle 111 \rangle$ direction.[2] One possible mechanism put forward for such giant enhancement in piezoelectric properties was the reorientation of the polar nanoregions (PNRs) within a compositionally disordered microstructure.[5] It was postulated that the reorientation of the PNRs creates a phase instability which in turn could lead to a greater electric-field-induced strain response.[6] However, subsequent observations showed that PNRs are not essential for this effect and similar effects can also be observed in normal ferroelectrics with no presence of PNRs or compositional disorder.[3,4] It was therefore realized that there should be an intrinsic crystallographic phenomenon responsible for the enhancement of electromechanical properties in ferroelectric crystals along nonpolar crystallographic directions.

Most well-known ferroelectrics are perovskite compounds with the general formula of ABO_3. The perovskite crystal structure is characterized by the archetype ferroelectric $BaTiO_3$, in which the Ba ions occupy the cell corners, O ions occupy the face centers, and the Ti ion is closest to the body center of the unit cell. Upon cooling below the ferroelectric Curie temperature T_C, $BaTiO_3$ undergoes a sequence of structural transitions from the cubic-to-tetragonal-to-orthorhombic-to-rhombohedral phases at successive lower temperatures. Within the framework of displacive phase transitions, the Ti ion is considered to be displaced from the center of the unit cell along the polarization direction of $\langle 001 \rangle$, $\langle 011 \rangle$, and $\langle 111 \rangle$ for the tetragonal, orthorhombic, and rhombohedral phases, respectively. The polarization vector can, however, be rotated away from its equilibrium direction upon application of an electrical field along certain nonpolar directions. Both first-principles and phenomenological calculations indicate that an easy rotation of the polarization vector for certain crystallographic axes ultimately leads to an electric-field-induced increased shear of the crystal lattice.[7–10] However, the microscopic mechanism through which polarization rotation might be related to an increased lattice deformation is unknown. Moreover, the standard model of polarization rotation raises additional concerns, such as whether the ferroelectric distortion in ABO_3 compounds is simply caused by an off centering of the B cation,[11] or how presumably reversible polarization rotation is related to experimentally observed *irreversible* electric-field-induced structural changes in the crystal symmetry.[3,12] Therefore, a fundamental understanding of the crystallographic effects of applied electric fields along nonpolar directions is required.

The central role of lattice dynamics towards the electromechanical properties of crystalline materials was originally recognized by Cochran.[13] From an atomistic viewpoint, the piezoelectric properties of crystalline solids result from a coupling between the specific vibration modes that are related to the elastic deformation of the lattice and to the generation of an electric dipole. In ferroelectric crystals, the former is connected to the long-wavelength acoustic phonons and the latter is connected to a soft transverse optic phonon mode near the Brillouin zone center.[14] Although an interaction between the transverse acoustic (TA) and the transverse optic (TO) modes exists in all piezoelectric ionic crystals, it is stronger when the frequencies of the two modes approach each other. This is observed in ferroelectric crystals for which the frequency of the transverse optic mode is low near the zone center or ZC ("soft" mode) and therefore partially overlaps with the acoustic mode, consequently leading to

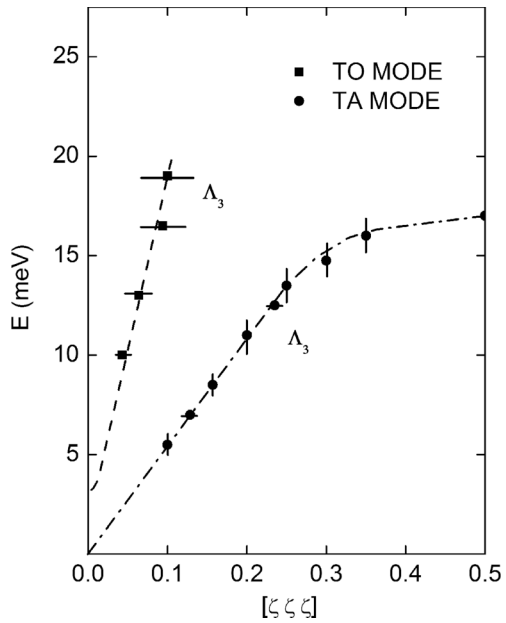

FIG. 1. Phonon dispersion curves for Λ_3 transverse acoustic (TA) and transverse optic (TO) branches in cubic $BaTiO_3$, after Harada *et al.* (Ref. 18).

high piezoelectric properties.[14–16] Therefore, the origins of enhanced piezoelectric properties in ferroelectric crystals for applied nonpolar electric fields can be understood by examining the induced changes in the TA and TO modes near the ZC.

$BaTiO_3$ was selected as the prototype material to undertake such a study. Particular phonon modes were investigated that could elucidate on induced lattice instabilities related to a higher piezoelectric response under application of electric fields along nonpolar directions.[10] Specifically, static electric fields of increasing magnitudes were applied along the nonpolar $[110]_{pc}$ direction of a tetragonal $BaTiO_3$ crystal and the electric-field-induced changes were examined for two vibrational modes near the 111 ZC that are correlated to the ferroelectric instability: namely, the transverse acoustic (TA) Λ_3 mode extending from the ZC to the R point (0.5,0.5,0.5) and the transverse optic (TO) Λ_3 mode which is the ferroelectric soft mode at the ZC.[17,18] The dispersion curves of these phonon modes for cubic $BaTiO_3$ over the entire Brillouin zone were published earlier and are reproduced here in Fig. 1. The naming convention for the particular modes follows from Refs. 18 and 19.

Here, we show that the application of an electric field along a nonpolar crystallographic direction leads to an upward shift in the energy of the Λ_3 TA branch. As a consequence, this branch is brought closer to the corresponding TO ferroelectric soft mode, thereby leading to an increased interaction between the long-wavelength TA and the soft-mode TO phonons for a range of wave vectors close to the ZC. This provides a direct microscopic mechanism for enhanced electromechanical coupling. The origin of such an electric-field-induced shift in the TA dispersion branch is subsequently examined within the context of order-disorder types of structural distortions in $BaTiO_3$.

The inelastic neutron scattering experiments were performed on the triple-axis spectrometer HB-3 at the High Flux Isotope Reactor of Oak Ridge National Laboratory. The inelastic spectrometer was operated with a fixed final energy of $E_f = 14.7$ meV. Pyrolytic graphite (PG) crystals were used as the monochromator and analyzer. The spectrometer was first set to a tight collimation mode of $48'-20'-20'-70'$ but was subsequently relaxed to $48'-40'-40'-120'$ to improve the signal-to-noise ratio. Two single crystals of $BaTiO_3$ obtained from different batches with dimensions of 10 mm $\times$ 1 mm $\times$ 1 mm were procured from MTI Corporation, CA, USA. The crystals were identically cut with faces normal to $\langle 110\rangle$ and $\langle 001\rangle$ pseudocubic directions, with 110 being the normal to the face with the larger surface area. The principal result is that of a stiffening of the TA branch, which is observed in both the crystals. Similar behavior in both samples supports that the observations reported here are intrinsic to $BaTiO_3$. For the neutron scattering experiments, the crystals were oriented in the *HHL* plane and electric field was applied normal to the 110 crystal face. Both constant-wave vector (Q) and constant-energy (E) scans were employed. The TA and TO phonon peaks for the Λ_3 modes were measured by scanning along the $[1+\zeta, 1+\zeta, -1+\zeta]$ direction from the $11\bar{1}$ Bragg peak, where $\zeta\zeta\zeta$ defines the reduced wave vector **q.** We note that the 111 direction is common to all tetragonal domain variants and therefore provides a practical advantage in terms of measuring phonons propagating along the $\zeta\zeta\zeta$ wave vector. All measurements were carried out under ambient conditions at room temperature.

Figure 2 shows the elastic scans at the ZC and the phonon spectra measured at constant energy transfer values of $\Delta E = 5$ and 7.5 meV, for the virgin state and at higher applied electric fields. As shown in Figs. 2(b) and 2(c), a shift in the peak positions for the TA Λ_3 mode to lower **q** values could be observed from the constant-E scans. This corresponds to an electric-field-induced stiffening of the TA phonon dispersion branch over an extended **q** range. In addition to peak shifts, a progressive dampening of the TO mode is also evident at higher electric fields. An anomalous broadening of both the TA and the TO modes is particularly evident from the constant-E scans at $\Delta E = 5$ meV. In comparison to the phonon peaks, the width of the elastic peak for $\Delta E = 0$ stays relatively unchanged with applied electric fields, as can be observed from Fig. 2(a).

The phonon peaks associated with the TA and the TO modes are fitted to Lorentzian profiles to extract the peak parameters. The TA dispersion branch over an extended **q** range is plotted in Fig. 3(a) for the zero field state and for $V = 1.5$ kV/mm (for $\Delta E = 5$ meV, the peak position is calculated for $V = 1.25$ kV/mm due to increased overlap between the modes at higher fields). The amounts of shift in **q** for the different constant-E scans are clear from the limited **q** range plots shown in Fig. 3(b). Figure 3(c) shows the shift in **q** as a percentage of the absolute $|\boldsymbol{q}|$ value at zero field. Although the shift in the TA dispersion is generally proportional to $|\boldsymbol{q}|$, there is an anomaly at $|\boldsymbol{q}| \sim 0.12$ where a dip in the relative shift is noted. In addition to peak shifts, the total intensity of the TA + TO phonon spectra also changed with increasing electric field, as shown in Fig. 3(d). The intensity change could reflect a more diffuse contribution of the modes to the dynamical structure

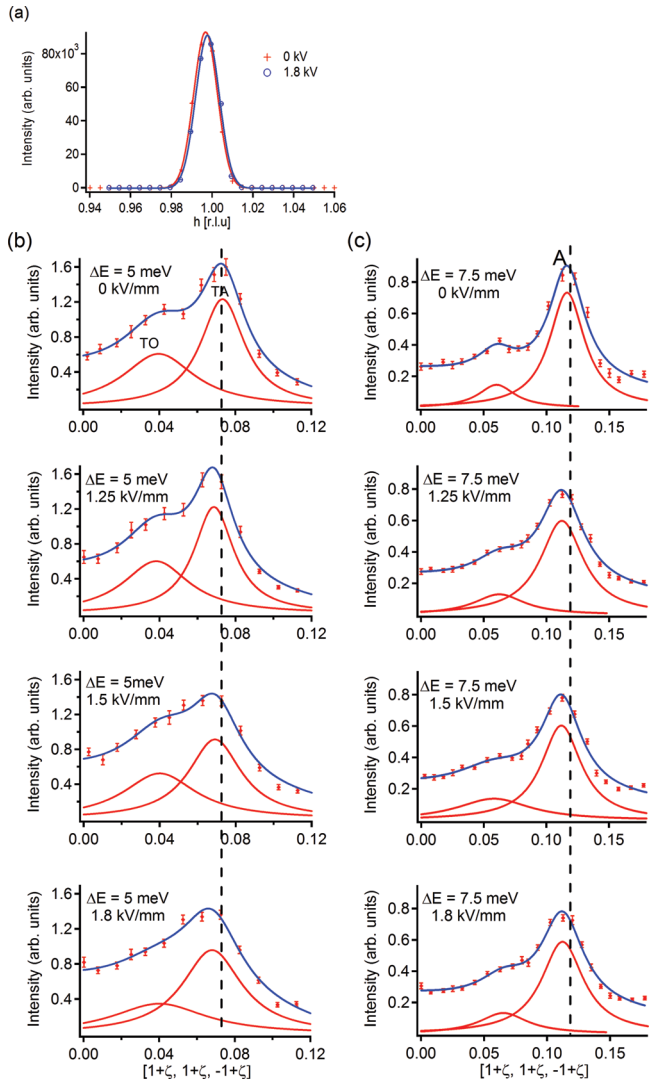

FIG. 2. (Color online) (a) Elastic scan near the ZC prior to and during the application of an electric field. (b), (c) Constant-energy scans along the $[1+\zeta, 1+\zeta, -1+\zeta]$ direction showing the peak positions for the Λ_3 TA and Λ_3 TO phonon modes: (b) Scans at $\Delta E = 5$ meV for fields of $V = 0$, 1.25, 1.5, and 1.8 kV/mm, respectively; (c) scans at $\Delta E = 7.5$ meV for fields of $V = 0$, 1.25, 1.5, and 1.8 kV/mm, respectively. Corresponding elastic scans for the 111 Bragg peak show no significant change in width upon electric field application.

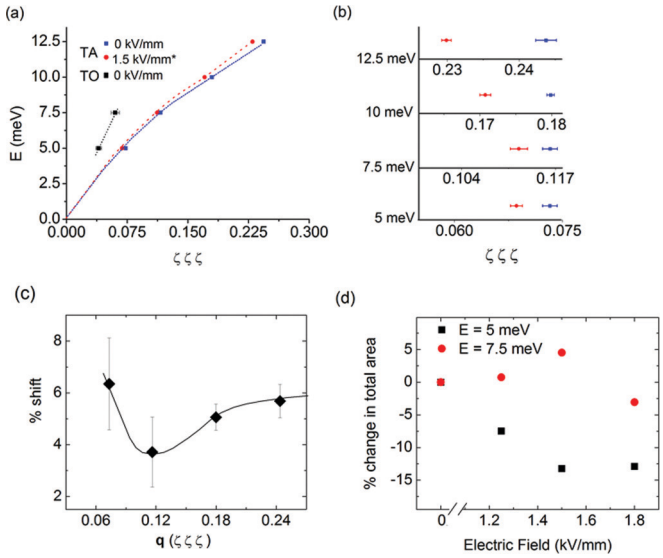

FIG. 3. (Color online) Electric-field-induced changes in phonon spectra: (a) The Λ_3 TA dispersion branch over an extended **q** range for zero field and for $V = 1.5$ kV/mm; the Λ_3 TO dispersion near the ZC is also shown for zero field; (b) the shift in TA peak positions can be observed for each ΔE; (c) the shifts in **q** for TA peaks are plotted as a percentage of the absolute **q** value at zero field; (d) percentage change in total peak area (TA + TO) as a function of applied electric field magnitude.

factor $S(\mathbf{Q}, E)$ or a quantum-mechanical interference between TA and TO modes, which we examine below.

The above features related to both anomalous peak profiles and dispersion of phonon modes at finite **q** values near the ZC can be expected as a consequence of coupling between the original eigenstates related to the TA and TO modes. Because of the electric-field-induced shift in the TA branch, a greater overlap of the two modes ensues. As the two phonon modes approach each other to have the same value of the wave vector **q**, a quantum-mechanical interference between the two competing scattering channels occurs.[17,18] If the modes are out of phase with respect to each other, the addition of the respective phonon peaks will result in a decrease of the total TA + TO peak intensity, as is observed in Fig. 3(d), and a redistribution of the spectral weight in the dynamical structure factor $S(\mathbf{Q}, E)$. Naturally, such coupling between an optic mode at $|\boldsymbol{q}| \approx \mathbf{0}$ and an acoustic mode dispersed in **q** will be largest near the ZC and will decrease with increasing **q**; this is observed from the constant-E scans in Figs. 2(b) and 2(c), where broadening is more apparent for phonon peaks at a lower energy transfer. The effects of a **q** dependent TA-TO mixing also causes an anomalous dispersion of acoustic phonons (such as shown in Fig. 1 of Ref. 20 by Shirane *et al.* for $PbTiO_3$), similar to a "dip" as observed in Fig. 3(c). In the case of $BaTiO_3$, additional anharmonic interference between TA and TO modes is also caused by a broadening of either mode and consequent overlap of their excitation spectra.[17,18] Therefore, the currently observed anomalous features in the phonon dispersions and peak profiles near the ZC are all consistent with the well-known effects of TA-TO mode coupling in ferroelectric crystals, which in turn is enhanced due to an electric-field-induced stiffening of the TA branch.

It is necessary to further examine the effects of TA-TO coupling at higher **q** values as we move away from the ZC. Although the extent of overlap between the TA and TO modes is less perceptive from the constant-E scans for higher **q** values, subtle effects of such mode coupling can be examined from changes in phonon lifetimes. It is intuitively understood that when two phonon modes overlap with each other, a single one phonon excitation of the lattice will decay into multiple correlated final phonon states; this will cause an accelerated decay of the original phonon excitation and will consequently cause a decrease in the phonon lifetimes. In order to examine this, we measured the energy distribution of the TA mode for different values of electric fields, by scanning across E with a constant $|\boldsymbol{q}| = 0.12$ (point A in Fig. 1), as shown in Fig. 4(a).

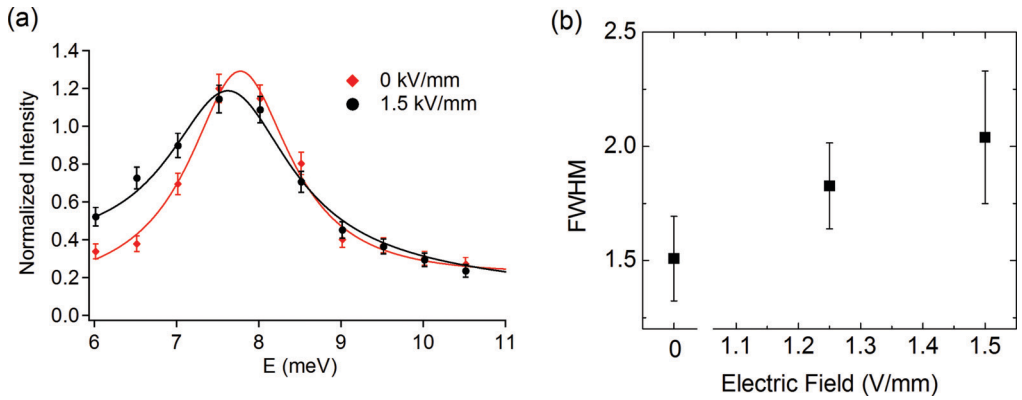

FIG. 4. (Color online) Effect of applied electric field on phonon linewidth: (a) Λ_3 TA phonon measured with a constant-Q scan for $I\mathbf{q}I = 0.12$ (point A in Fig. 1), at zero field and $V = 1.5$ kV/mm; (b) field dependence of the TA peak width presented as FWHM.

The full width at half maxima (FWHM) for the phonon peaks at different applied field amplitudes are obtained from Lorentzian fits and are plotted in Fig. 4(b). There is a steady increase in FWHM with electric field amplitude, implying a decrease in the phonon lifetime. The broadening of the TA phonons cannot be attributed to changes in the domain structure since no apparent broadening of the elastic peak at ZC can be observed [Fig. 2(a)]. Instead, it is most likely that the decrease in phonon lifetimes is due to an increased coupling between the TA and TO phonons. The implication is that the electric-field-induced enhanced TA-TO interaction is existent for phonons with a rather broad range of wave vectors **q**.

It is worthwhile to mention here that calculations based on Landau-Devonshire-Ginzburg (LGD) type phenomenological theories indicates that the enhanced piezoelectric properties along nonpolar directions in ferroelectric crystals could be related to a softening of the transverse dielectric coefficient.[9,21] However, unlike the *dielectric* coefficient, the current results indicate no such role for the transverse *elastic* constant. On the contrary, a hardening of the TA mode would be consistent with an increase in the elastic constant under a nonpolar electrical bias. In the following, we examine why a hardening of the TA mode could occur in $BaTiO_3$ under applied electric fields along a nonpolar direction.

Lattice distortions in $BaTiO_3$ have been described to have both displacive and order-disorder characteristics.[13,22] In the order-disorder case, $BaTiO_3$ can be described to be intrinsically disordered with the Ti ions displaced along either of the ⟨111⟩ directions. Depending on how the localized distortions are correlated along the different crystallographic directions, the macroscopic symmetry could be either cubic, tetragonal, rhombohedral, or orthorhombic.[22] In $BaTiO_3$, the displacement of the Ti ions against the oxygen ions along Ti-O-Ti chains dominates the ferroelectric instability at the Γ point.[23] Consequently, the dispersion of the TA Λ_3 mode is dependent on the degree of correlation between the different localized displacements of Ti—a steeper dispersion is expected from strongly correlated Ti displacements along the Ti-O-Ti chains.[23,24] It is therefore conceivable that when an electrical bias is applied along the $[110]_{pc}$ direction, the correlation among the localized Ti displacements along a specific crystallographic axis is increased and is responsible for "hardening" of the TA dispersion branch.

Finally, we observe that the shift in the TA phonon dispersion persists even subsequent to the withdrawal of the electric field (Fig. 5). This could indicate a permanent change in the atomic arrangements. An irreversible electric-field-induced lattice distortion in $BaTiO_3$, for fields applied along nonpolar crystallographic directions, is in line with previous observations of permanent changes in crystal symmetry in $BaTiO_3$ single crystals.[3,12] While the intrinsic disorder for atomic displacements in $BaTiO_3$ has been described as essentially a dynamic phenomenon,[18] it is also possible that an ordered phase is indeed induced upon application of an electrical bias.[7] The latter view is supported from the present results. Additional insights in this area can be gained from diffuse scattering measurements under applied electric fields.

The current study shows the significance of *in situ* neutron spectroscopy characterization of phonons towards identifying the microscopic phenomena that can potentially lead to giant electromechanical properties in solids. The key phenomenon observed here is an increase in TA-TO coupling with an electric field application, which likely originates from changes in chainlike correlations among individual atomic displacements. A clearer understanding of the nature of

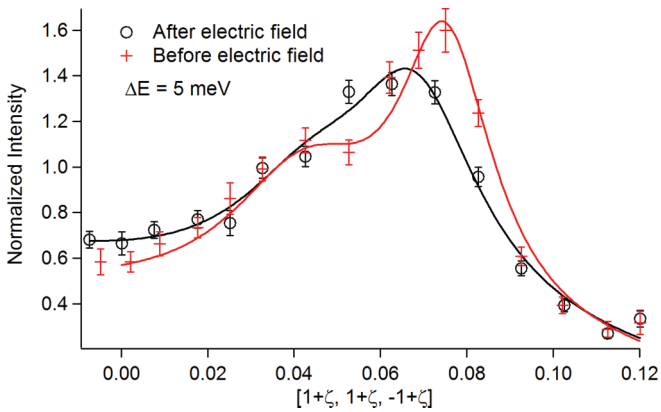

FIG. 5. (Color online) Irreversible change in the phonon spectra for $\Delta E = 5$ meV before and subsequent to the application of electric fields.

intermixing among the different phonon modes is expected from detailed linewidth analyses of phonon spectra measured under applied electric fields. For some other types of correlated structural changes in perovskite oxides, such as cooperative tilts of oxygen octahedra[25,26] and changes in compositional disorder among the different atomic sites,[6] their individual effects on electromechanical coupling properties needs further investigation. In the specific case of relaxors, it remains particularly unclear whether the enhanced electromechanical coupling for nonpolar directions is mainly due to an increased TA-TO coupling[27] or due to a stronger coupling of TA phonons with microscopic features such as PNRs.[6] Therefore, an understanding of how the different structural changes affect the acoustic and optic phonon modes *during* electric field application will be critical for the development of emerging relaxors and nonlead ferroelectrics with high electromechanical properties.

Research conducted at ORNL's High Flux Isotope Reactor was sponsored by the Scientific User Facilities Division, Office of Basic Energy Sciences, US Department of Energy. A.P. acknowledges funding from a Laboratory Directed Research and Development Fund of Oak Ridge National Laboratory. O.D. acknowledges support by the U.S. Department of Energy, Basic Energy Sciences, Materials Sciences and Engineering Division. The authors also acknowledge technical assistance from Christopher M. Redmon and Daniel Maierhafer on the high voltage experimental setup.

*Corresponding author: abhijit.pramanick@gmail.com

[1] K. Uchino, *Piezoelectric Actuators and Ultrasonic Motors* (Kluwer Academic, Boston, 1996).
[2] S.-E. Park and T. R. Shrout, J. Appl. Phys. **82**, 1804 (1997).
[3] S. Wada, K. Yako, H. Kakemoto, T. Tsurumi, and T. Kiguchi, J. Appl. Phys. **98**, 014109 (2005).
[4] S. Wada, K. Takeda, T. Muraishi, H. Kakemoto, T. Tsurumi, and T. Kimura, Jpn. J. Appl. Phys. **46**, 7039 (2007).
[5] G. Xu, Z. Zhong, Y. Bing, Z.-G. Ye, and G. Shirane, Nat. Mater. **5**, 134 (2006).
[6] G. Xu, J. Wen, C. Stock, and P. M. Gehring, Nat. Mater. **7**, 562 (2008).
[7] H. Fu and R. E. Cohen, Nature (London) **403**, 281 (2000).
[8] D. Damjanovic, J. Am. Ceram. Soc. **88**, 2663 (2005).
[9] M. Davis, M. Budimir, D. Damjanovic, and N. Setter, J. Appl. Phys. **101**, 054112 (2007).
[10] M. Budimir, D. Damjanovic, and N. Setter, Phys. Rev. B **73**, 174106 (2006).
[11] R. E. Cohen, Nature (London) **358**, 136 (1992).
[12] H. Cao, C. P. Devreugd, W. Ge, J. Li, D. Viehland, H. Luo, and X. Zhao, Appl. Phys. Lett. **94**, 032901 (2009).
[13] W. Cochran, Adv. Phys. **9**, 387 (1960).
[14] V. Dvorak, Phys. Rev. **167**, 525 (1968).
[15] D. G. Sannikov, Sov. Phys. Solid State **4**, 1187 (1962).
[16] B. D. Silverman and R. I. Joseph, Phys. Rev. **129**, 2062 (1963).
[17] G. Shirane, J. D. Axe, J. Harada, and A. Linz, Phys. Rev. B **2**, 3651 (1970).
[18] J. Harada, J. D. Axe, and G. Shirane, Phys. Rev. B **4**, 155 (1971).
[19] R. A. Cowley, Phys. Rev. **134**, A981 (1964).
[20] G. Shirane, J. D. Axe, J. Harada, and J. P. Remeika, Phys. Rev. B **2**, 155 (1970).
[21] M. Budimir, D. Damjanovic, and N. Setter, J. Appl. Phys. **94**, 6753 (2003).
[22] R. Comes, M. Lambert, and A. Guinier, Acta Crystallogr., Sect. A **26**, 244 (1970).
[23] P. Ghosez, E. Cockayne, U. V. Waghmare, and K. M. Rabe, Phys. Rev. B **60**, 836 (1999).
[24] P. Sc. H. Ghosez, X. Gonze, and J. P. Michenaud, Ferroelectrics **206**, 205 (1998).
[25] I. Levin and I. M. Reaney, Adv. Funct. Mater. **22**, 3445 (2012).
[26] I. Tomeno, J. A. Fernandez-Baca, K. J. Marty, K. Oka, and Y. Tsunoda, Phys. Rev. B **86**, 134306 (2012).
[27] J. Hlinka, S. Kamba, J. Petzelt, J. Kulda, C. A. Randall, and S. J. Zhang, Phys. Rev. Lett. **91**, 107602 (2003).